Environmental Pollution 244 (2019) 534–548

Contents lists available at ScienceDirect

Environmental Pollution

journal homepage: www.elsevier.com/locate/envpol

Sodium fluoride induced skeletal muscle changes: Degradation of proteins and signaling mechanism☆

P. Sudheer Shenoy [a, *], Utsav Sen [a, 1], Saketh Kapoor [a, 1], Anu V. Ranade [b], Chitta R. Chowdhury [c, d], Bipasha Bose [a, **]

[a] Stem Cells and Regenerative Medicine Centre, Yenepoya Research Centre, Yenepoya Deemed to be University, University Road, Mangalore, 575018, Karnataka, India
[b] College of Medicine, University of Sharjah, United Arab Emirates
[c] Department of Oral Biology & Genomic Studies, A.B.Shetty Memorial Institute of Dental Sciences, Nitte University, Mangalore, 575018, Karnataka, India
[d] School of Health and Life Sciences, Biomedical and Environmental Health Group, De Montfort University, Leicester, United Kingdom

ARTICLE INFO

Article history:
Received 7 June 2018
Received in revised form
4 October 2018
Accepted 5 October 2018
Available online 10 October 2018

Keywords:
Sodium fluoride (NaF)
Parts per million (ppm)
C2C12
Myoblasts
Differentiation
Myotubes
Hypertrophy
Atrophy

ABSTRACT

Fluoride is a well-known compound for its usefulness in healing dental caries. Similarly, fluoride is also known for its toxicity to various tissues in animals and humans. It causes skeletal fluorosis leading to osteoporosis of the bones. We hypothesized that when bones are affected by fluoride, the skeletal muscles are also likely to be affected by underlying molecular events involving myogenic differentiation. Murine myoblasts C2C12 were cultured in differentiation media with or without NaF (1 ppm-5 ppm) for four days. The effects of NaF on myoblasts and myotubes when exposed to low (1.5 ppm) and high concentration (5 ppm) were assessed based on the proliferation, alteration in gene expression, ROS production, and production of inflammatory cytokines. Changes based on morphology, multinucleated myotube formation, expression of MyHC1 and signaling pathways were also investigated. Concentrations of NaF tested had no effects on cell viability. NaF at low concentration (1.5 ppm) caused myoblast proliferation and when subjected to myogenic differentiation it induced hypertrophy of the myotubes by activating the IGF-1/AKT pathway. NaF at higher concentration (5 ppm), significantly inhibited myotube formation, increased skeletal muscle catabolism, generated reactive oxygen species (ROS) and inflammatory cytokines (TNF-α and IL-6) in C2C12 cells. NaF also enhanced the production of muscle atrophy-related genes, myostatin, and atrogin-1. The data suggest that NaF at low concentration can be used as muscle enhancing factor (hypertrophy), and at higher concentration, it accelerates skeletal muscle atrophy by activating the ubiquitin-proteosome pathway.

1. Introduction

Fluorine/Fluoride (Fl/F) is a highly electronegative and extremely reactive compound, and its levels in drinking water should not exceed 1.0 mg/L (1 ppm- Parts per million) (WHO, 2008). However, high fluoride levels (˃3 ppm) are present in water in fluorosis endemic areas and it has been reported that the source of natural fluoride is rocks and granulites (Dharmagunawardhane et al., 2016; Tsunogae et al., 2003). In addition to fluoride in nature, the human population is also exposed to fluoride mainly through drinking water, fluoride rich natural foodstuffs; fluoride supplemented marketed food, fluoridated dentifrices, fluoride varnish including fluoride mouth wash. Fluoride is also considered as an important beneficial element in human health, since it has an anti-carieogenic effect and maintenance of bone density. Therefore, the diet and drinking water contributes to approximately 0.05 mg/kg daily intake for an adult individual. Such a dose (0.5 mg/kg/day) can help reduce the rate of dental caries in humans. Fluoride reportedly exerts both positive and negative effects on human health (Edmunds and Smedley, 1996; Urbansky, 2002; Bailey et al., 2006; Nielsen, 2009).

Exposure to fluoride at low concentrations causes growth, development and maintenance of the skeletal systems

☆ This paper has been recommended for acceptance by Dr. D Carpenter.
* Corresponding author.
** Corresponding author.
E-mail addresses: shenoy@yenepoya.edu.in, shenoy2000@yahoo.com (P.S. Shenoy), Bipasha.bose@yenepoya.edu.in, Bipasha.bose@gmail.com (B. Bose).
[1] Equally contributing second authors.

https://doi.org/10.1016/j.envpol.2018.10.034
0269-7491/

(Antonarakis et al., 2014; O'Mullane et al., 2016). Chronic and acute exposure to fluoride causes dental mottling, skeletal fluorosis (Krishnamachari, 1986; Kebede et al., 2016; Denbesten and Li, 2011; Asawa et al., 2015) and non-skeletal fluorosis such as musculoskeletal disorders (Shashi, 1989; Shashi et al., 1992; Shashi et al., 2010; Shashi and Rana, 2016). Besides, neuronal (Ge et al., 2006; Zhang et al., 2008) and gastrointestinal (Muller et al., 1992; Buzalaf and Whitford, 2011), liver (Dabrowska et al., 2006; Pereira et al., 2013) and renal (Antonio et al., 2017; Zohoori et al., 2015), reproductive (Wang et al., 2017; Yin et al., 2015; Zhang et al., 2016) disorders are also caused by fluorosis. Furthermore, fluorosis also affects the antioxidant system in the body (Mukhopadhyay and Chattopadhyay, 2014; Feng et al., 2015).

Skeletal fluorosis is often associated with skeletal muscle fluorosis (non-skeletal fluorosis). Muscle is a sensitive organ that is susceptible to fluoride induced damage in chronic fluoride toxicity resulting in functional changes manifested as muscle ache and weakness due to the alterations in the levels of serum lactate dehydrogenase (LDH) (Li et al., 1989). Fluorosis causes musculoskeletal damage and destroys collagen structure in muscles, tendons, ligaments and bone. Fluorosis reportedly led to gross alteration in the histological structure and function of gastrocnemius muscle (Shashi and Rana, 2016; Chinoy and Memon, 2001; Shashi et al., 2009). Fluoride toxicity destroys the structure and functions of actin and myosin filaments of skeletal muscle areas by degeneration (Shashi, 1989; Shashi et al., 1992; Park et al., 1999). Histological analysis had shown that skeletal muscle fluorosis causes changes such as apoptosis and necrosis of muscle fibres and retraction of muscle fibres from the perimysial sheath. The results of the in-vivo studies indicated that mitochondria and myofibrils are damaged in skeletal muscle by fluoride. Fluorosis *in vivo* led to a decrease in the activities of mitochondrial enzymes such as succinate dehydrogenase, cytochrome oxidase, and Mg^{2+} adenosine triphosphatase, causing impairment of energy metabolism leading to skeletal muscle necrosis (Pang et al., 1996).

Skeletal muscle is a dynamic tissue and is highly adaptable and responds to the daily wear and tear (biochemical and biophysical signals). Skeletal muscle can increase its mass, i.e., hypertrophy during development, exercise, stretch and mechanical loading (Sharples and Stewart, 2011). Furthermore, physiologically hypertrophy in skeletal muscle can also be achieved by blocking myostatin (GDF-8; negative regulator of muscle mass) (Sharples and Stewart, 2011); or using supplements such as betaine (Senesi et al., 2013), resveratrol (Montesano et al., 2013). Other factors such as Insulin-like growth factor-1 (IGF-1) promotes skeletal muscle hypertrophy through its interaction with IGF-1R by activating AKT and phosphatidylinositol-3,4,5-triphosphates (PIP3) (Sartorelli and Fulco, 2004; Sandri, 2008; Glass, 2005). AKT, in turn, enables the downstream kinase mTOR, which stimulates p70S6 kinase and other effectors, resulting in increased protein synthesis (Sandri, 2008; Glass, 2005). On the other hand, skeletal muscle atrophy or severe loss of muscle mass is observed during ageing, disuse and other catabolic diseases such as cancer, AIDS, congestive heart failure, COPD, arthritis and sarcopenia. During skeletal muscle atrophy increased protein degradation may occur due to changes in hormones such as IGF-1, testosterone, glucocorticoids. Furthermore increase in levels of TGF-β, myostatin and cytokines such as TNF-α, IL-6 (Sharples and Stewart, 2011), TWEAK and TRAF6 (Kumar et al., 2012) can also cause muscle atrophy. Oxidative stress, ROS production and decreased amino acid availability are also reported to result in muscle atrophy (Sharples and Stewart, 2011).

Fluorosis induced skeletal muscle hypertrophy and hyperplasia in rabbits and rats in low concentrations and atrophy at higher concentrations (Shashi, 1989; Shashi et al., 2010). However, the underlying mechanisms of fluoride induced skeletal muscle hypertrophy and atrophy ***in vitro*** and ***in vivo*** is not clear. In this study, hence, we have assessed the effects of sodium fluoride (NaF) on C2C12 murine myoblasts cell line *in vitro*. Our results show that NaF at lower concentration causes proliferation of myoblasts and hypertrophy of the myotubes by activating IGF-1 signaling pathway and at higher concentration; it causes atrophy of myotubes by activating ubiquitin-proteosome pathway.

2. Material and methods

2.1. Cell culture

C2C12 mouse myoblast cell line was cultured in DMEM (Dulbecco modified Eagle medium) high glucose supplemented with 20% (v/v) FBS (Fetal Bovine Serum), 1% penicillin & streptomycin and 1% L-glutamine (all from Gibco, Thermo Fisher scientific Carlsbad, CA, USA) up to 70% confluence at 37 °C and 5% CO_2. Once the cells reached desired confluence, the medium was changed to differentiation medium, DMEM supplemented with 2% horse serum (Gibco, Thermo Fisher scientific Carlsbad, CA, USA) to induce differentiation.

2.2. Cell proliferation assay

To show the direct effects of NaF on C2C12 myoblast proliferation, myoblasts were seeded at a density of 6000 cells/cm^2 in growth medium on 96-well microtitre plates overnight. Exogenous NaF was added to the cells, and cultured for 72 h. Cell number was assessed using MTT assay according to the published protocols (Oliver et al., 1989).

2.3. Cell growth and viability

In order to test the cell growth and viability of C2C12 myoblast in the presence and absence of NaF, cells were plated in 35 mm culture dishes at 40% confluence in growth medium with (1 ppm, 1.5 ppm, 5 ppm) or without NaF for 72 h. Cell growth and viability were calculated using trypan blue exclusion method; cells were trypsinized and counted with the help of hemocytometer (Senesi et al., 2013; Montesano et al., 2013). Cells were observed under the microscope and images were captured. Cells cultured in proliferation media and differentiation media without NaF were used as controls.

2.4. Myoblast differentiation and Myotube formation

C2C12 myoblast cells were seeded in 6 well plates and allowed to attach overnight. The culture medium was replaced with differentiation medium containing with or without NaF and cultured for 24 h, 48 h, 72 h and 96 h. At the end of each time point, the cells were fixed with 4% PFA and stained with Giemsa (Sigma USA) according to the standard protocol. Cell morphology was observed by phase contrast microscopy using Primovert (Carl Zeiss, Germany) with camera attachment and images were captured using Zen lite software (Carl Zeiss, Germany).

2.5. Immunofluorescence

Differentiated (myotubes) and undifferentiated myoblasts were cultured with or without NaF in 8 well chamber slides (Eppendorf Germany). The cells were fixed in freshly prepared 4% paraformaldehyde and permeabilized with 0.3% Triton X100 (Sigma) in PBS. The non-specific binding sites were blocked with 5% normal donkey serum (Sigma) in PBS for 1 h and incubated overnight at

4 °C with primary antibodies, followed by appropriate secondary antibody for 1 h, counterstained with mounting media (ProLong Gold Antifade, Thermo Fisher, USA) containing DAPI. The slides were observed, and images were captured under ZOE Fluorescent cell imager (Bio-Rad, USA). Detailed list of antibodies and their respective dilutions can be found in the Supplementary Table 1.

2.6. Characterization of myotubes treated with or without NaF

Myotubes containing more than or equal to three nuclei were considered for counting the total number of myotubes per field, myonuclei and myotubes area measurements (Velica and Bunce, 2011). The myotube area was measured using the Image J software and represented as μm^2. The graph was plotted by taking the average myotube area of 10 random fields, and values are represented as mean ± SD.

The myotube diameter was evaluated after immunostaining the myotubes with MyHC1 antibody and DAPI using Image J software, three measurements of the diameter were taken along each myotube, in at least ten different fields, for at least 100 myotubes per culture.

The myogenic fusion index was calculated after immunostaining with MyHC1 antibody and DAPI, as the ratio between the number of nuclei in multinucleated myotubes and the total number of nuclei in a given field. 400 to 700 nuclei were counted per culture in at least ten different fields.

2.7. Detection ROS generation in C2C12 using fluorescence emission

C2C12 were cultured in the presence and absence of NaF and were tested for the presence of ROS generation, DCFDA-2', 7'–dichlorofluorescin diacetate (Sigma, USA) (cell permeant reagent) a fluorogenic dye that measures hydroxyl, peroxyl and other ROS activity within the cell. Briefly, C2C12 cells were plated in 96 well plates in growth media at 6000 cells/well. After overnight attachment of the cells; they were treated with different concentrations of NaF in differentiation media. At the end of 24 h time point, the media was removed, and the cells were incubated with 5 μM of DCFDA in PBS for 30 min at 37° C with 5% CO_2. After incubation, the dye was removed, and 200 μl of differentiation media was added in each well. Fluorescence was measured at various time points using multimode fluorescent plate reader FLUOstar Omega (BMG LABTECH, Germany) at 485/535 nm respectively (Rosenkranz et al., 1992).

2.8. Detection of ROS generation in myotubes by fluorescence microscopy

C2C12 cells were cultured in 8 well-chambered cover slips (Eppendorf) in the growth media at a cell density of 10,000 cells/well and allowed to attach overnight. After attachment of the cells, a time course myogenic differentiation (24 h, 48 h, 72 h, and 96 h) was done by treating the cells with different concentrations of NaF in differentiation media. At the end of each time point, the cells were processed as mentioned in the previous experiment, the green fluorescently stained cells (ROS positive) were observed with ZOE fluorescent cell imager (BIO-RAD, USA) and the images were captured and analyzed (Sriram et al., 2011).

2.9. Quantitative real time-PCR (RT-PCR)

Total RNA was extracted from myoblasts and myotubes treated with or without NaF using RNeasy mini kit (Qiagen 74104). cDNA was reverse transcribed using iScript RT (BioRad 1708891), and subsequently, quantitative PCR was performed using SsoFast™ Eva Green super mix (BioRad 1725201), as per manufacturer's instructions. Gene expression was carried out for a wide variety of markers such as cyclins, myogenic regulatory factors, MyHC1 and mitochondrial genes upon exposure to NaF on C2C12 myotubes. Transcript levels were normalized to GAPDH, with relative gene expression fold-change calculated using $2^{(-\Delta\Delta Ct)}$ method [threshold cycle (Ct) values]. The list of primers used can be found in the Supplementary Table 2.

2.10. Immunoblotting/western blot

Myoblasts and myotubes treated with or without NaF were dissolved in protein lysis buffer containing [50 mM Tris, (pH 7.5), 250 mM NaCl, 5 mM EDTA, 0.1% NP-40, protease inhibitor cocktail (Sigma-Aldrich P2714), 2 mM NaF, 1 mM Na3V04, and 1 mM phenylmethylsulfonylfluoride (PMSF)], incubated for 15 min and then centrifuged at 12,000 rpm for 10 min. The supernatant was taken for further analysis, and proteins were quantified using Bradford reagent (Bio-Rad). 20 μg of protein lysate was run on SDS-PAGE, using a 10–12% gel, and the proteins were transferred to nitrocellulose membrane. The membrane was then blocked for 1 h in 5% milk in 1× Tris buffered saline-Tween 20 (TBST), and then incubated overnight with specific primary antibodies with 5% milk in 1xTBST. The membrane was washed in 1× TBST for 5 min (5 times) and then incubated with HRP-conjugated secondary antibodies. Bands were visualized using enhanced chemiluminescence method (Advansta, USA) and detected using X-Ray film. Quantitative measurement of the bands was performed by densitometric analysis using LiCor Image Studio Lite, Version 5.2 software.

2.11. Flow cytometry

Myoblasts and myotubes treated with or without NaF were washed with PBS and fixed with ice-cold 4% PFA in PBS. The cells were then permeabilized with 0.3% Triton X-100, incubated with primary antibody for 1 h followed by incubation with fluorescence-conjugated secondary antibody for 30 min (antibody details are given in Supplementary Table 1). The antibody stained cells (10,000 events) were then acquired on Guava easyCyte (Merck Millipore USA) flow cytometer using Guava InCyte software. Flow cytometric analysis was carried out using deNovo FCS Express software, USA.

2.12. Statistical analysis

Data was analyzed by using two tailed Student's *t*-test to determine the statistically significant measurement. The differences between more than two groups were analyzed by ANOVA. The *P* values of $P \leq 0.05$ (*) and $P \leq 0.01$ (**) were considered as significant. Error bar represents the ±standard error of mean.

3. Results

3.1. Effect of NaF on the proliferation of C2C12 myoblast cells

C2C12 mouse myoblasts were cultured in proliferation media (Fig. 1A) and allowed to grow up to 70% confluency. The cells at this stage were immunostained with MyoD antibody (Fig. 1A) to confirm the undifferentiated state of the myoblasts. Initially, proliferating C2C12 myoblast cells were screened for NaF toxicity at a concentration from 1 ppm to 40 ppm. At this broad range (1 ppm-40 ppm), NaF promoted proliferation of the myoblasts without any cell death (Fig. S1A). Cell viability decreased only above 40 ppm, and cell death was seen (Fig. S1B).

With these observations, C2C12 in the proliferative phase were exposed to different concentration of NaF (1 ppm, 1.5 ppm and

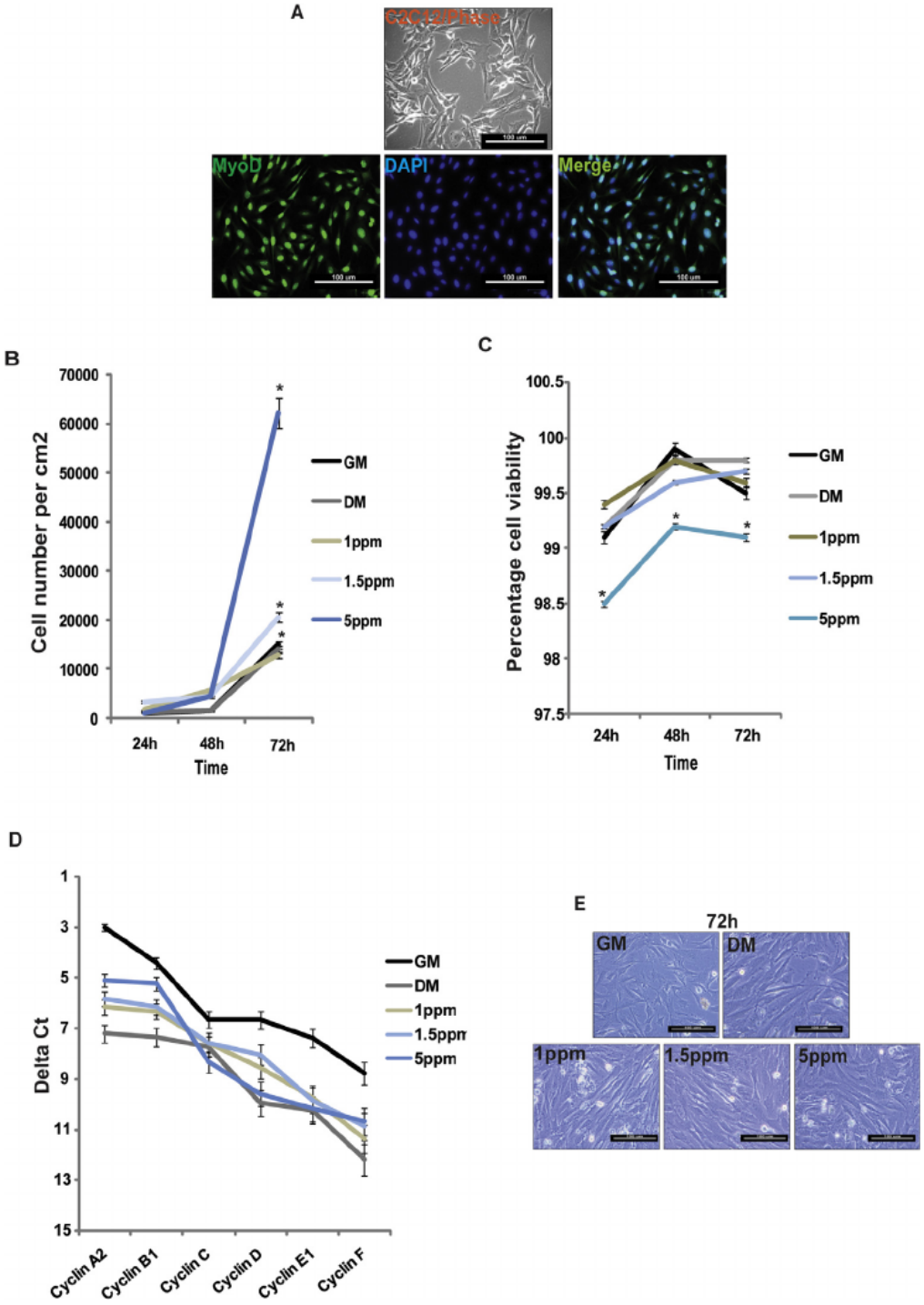

Fig. 1. Proliferation and the inhibitory effect of NaF on C2C12 cells: Cells were cultured in growth medium and differentiation medium in the presence and absence of NaF. **A)** Phase contrast and immunofluorescence images of C2C12 cells stained with MyoD antibody cultured in growth medium. **B)** The proliferation of C2C12 cells (growth curve) in the presence of different concentrations of NaF (1 ppm, 1.5 ppm, 5 ppm) *P 0.05. **C)** Cell viability assay conducted on C2C12 cells in the presence of different concentrations of NaF (1 ppm, 1.5 ppm, 5 ppm) *P 0.05. **D)** Expression (qRT-PCR) pattern of different cyclins at 24 h after the cells were treated with different concentrations of NaF. **E)** Phase contrast images of C2C12 cells captured after 72 h of proliferation and morphological changes were observed after NaF treatment. Values are means of ±SD of three experiments. Scale bars: 100 μm.

5 ppm) at 24 h, 48 h, and 72 h time points. Initially up to 24 h of NaF treatment, C2C12 cells proliferated steadily, and the proliferation rated increased at 48 h and attained a peak at 72 h (Fig. 1B). Cells treated with 1 ppm exhibited higher proliferation when compared to untreated controls (Growth media control-GM control). Treatment with 1.5 ppm and 5 ppm of fluoride displayed no inhibition in the proliferation of myoblasts when compared to untreated cells (Fig. 1B). 5 ppm of NaF treatment induced significantly high proliferation rate in the C2C12 myoblasts when compared to other doses (Fig. 1B). Negligible cell death was observed in trypan blue viability assay in all the NaF treated doses including untreated controls thereby confirming the cell death in the permissible cell culture turnover of proliferating myoblasts (Fig. 1C).

In addition to high proliferation rate of C2C12 in the presence of NaF, obtained in the growth curve, significant downregulated expression of cyclin genes were observed in qRT-PCR performed at 24 h of proliferation in the presence and absence of NaF indicating that the cells have exited the cell cycle (Fig. 1D). Further, morphology shift from cuboidal (undifferentiated) to spindle shaped was observed upon exposure of the C2C12 cells to different concentrations of NaF thereby indicating the readiness of the cells for differentiation (Fig. 1E). We also investigated the role of NaF on initiation of differentiation, using qRT-PCR gene expression analysis of the two principal myogenesis regulatory factors (MRFs) *MyoD* and *Myf5* (Fig. 2A and B). There was significant upregulation of *MyoD* and *Myf5*; this might be due to excessive proliferation of the cells at the given concentration of NaF (Kitzmann and Fernandez, 2001; De Falco and De Luca, 2006; Berkes and Tapscott, 2005). Downregulation of these MRFs were only observed in the C2C12 cells cultured only in differentiation medium. Moreover, the differentiation marker *MyoG* exhibited an upregulation in the C2C12 cultures in differentiation media bearing a direct correlation with the increasing dose of NaF (Fig. 2C).

3.2. Effect of NaF on the production of reactive oxygen species (ROS) in C2C12 myoblast cells

Production of ROS or oxidative stress induces skeletal muscle atrophy, cachexia, and sarcopenia (Li and Reid, 2000; Gomes-Marcondes and Tisdale, 2002; Mantovani et al., 2004; Moylan and Reid, 2007). We observed the effect of NaF on ROS production in C2C12 myoblast cells. NaF increased the ROS production in a dose-dependent manner (0 ppm, 1 ppm, 1.5 ppm, 5 ppm), and 5 ppm concentration showed maximum ROS production (Fig. 2D). NaF also induced ROS production in differentiating C2C12 myotubes in a time dependent manner. ROS production was significantly increased at 48 h with the addition of NaF at a concentration of 1 ppm and attained a peak at a concentration of 1.5 ppm (Fig. 2D and E). ROS production decreased at NaF concentration of 5 ppm; this might be due to myotube atrophy and also due to decrease in myotube number (Fig. 2D and F). ROS production decreased with time and was lowest at 72 h (Fig. 2D and E). ROS production at different concentrations correlated well with the fluorescence microscopy observations.

3.3. NaF induced ROS production leading to mitochondrial damage in C2C12 myotubes

Excessive production of ROS is detrimental to the cells because of its effects on lipids, proteins, and DNA (Xiao et al., 2017). Our studies indicated that NaF caused ROS production both in myoblast and myotubes which resulted in excessive mitochondrial damage beyond repair. We, hence, investigated the expression of genes controlling the mitochondrial dynamics in C2C12 myotubes to different concentrations of NaF. *Parkin (Park-2),* a mitochondrial E3 ligases and *Drp1* (Dynamin-like protein 1) promoting the fragmentation of mitochondria were significantly upregulated in C2C12 myotubes treated with NaF at 1.5 ppm (Fig. S1C). This indicated that ROS might act as a trigger for the induction of *Parkin*-dependent mitophagy (Xiao et al., 2017). Expression of *Mfn2 (coordinates mitochondrial fusion), and Pink1 (Park6)* was completely absent in all NaF treatments (Fig. S1C). Other factors such as *Mfn1*, *March5*, *Fis1, and BNIP3 were also* expressed (Fig. S1C).

3.4. NaF caused expression of inflammatory cytokines in C2C12 myoblasts

We wanted to investigate if NaF induced ROS production can cause an increase in inflammatory cytokine expression. qRT-PCR gene expression analysis indicated a time-dependent increase in various inflammatory cytokines such as IL-6 and TNF-α gradually starting from 24 h to 72 h (Fig. 3A and B). Out of these three concentrations of NaF tested for this study, 1.5 ppm at 72 h increased the expression of IL-6 by two folds (Fig. 3A) and TNF- α by four folds (Fig. 3B). However, both the other concentrations of NaF-1.5 ppm and 5 ppm resulted in the decrease of TNF- α (2 fold), as compared to untreated controls (Fig. 3B).

3.5. Low and high concentrations of NaF respectively induced and inhibited myogenic differentiations

Next, we studied the myogenic differentiation of C2C12 cells cultured in differentiation medium (2% HS) in the presence and absence of NaF. A time course myogenic differentiation was conducted in the presence of NaF at a concentration of 0 ppm, 1 ppm, 1.5 ppm, and 5 ppm for four days (96 h). At the end of 96 h the differentiated myotubes were fixed and stained with Giemsa (Fig. 3C), simultaneously the myotubes were fixed and immunostained with MyHC-1 (Fig. 3D). The myotubes were analyzed for number of myotubes per field (Fig. 3E) and number of nuclei per myotube (Fig. 3F). NaF at a concentration of 1 ppm had no effect on myotubes, number of myotubes (08/field) (Fig. 3D and E) and myonuclei ($\approx$40) and therefore, appeared similar to that of untreated control (Fig. 3F). This indicated that the C2C12 underwent normal myogenesis/myogenic differentiation in presence of 1 ppm of NaF, which is indeed a safe dose in drinking water for humans. However, at NaF concentration of 1.5 ppm, the number of myotubes decreased to 06 per field (Fig. 3D and E) but the number of myonuclei per myotube increased ($\approx$50) indicating enhanced myogenesis (Fig. 3F) when compared to untreated control and 1 ppm treatments. Furthermore, at NaF at a dose 5 ppm, the number of myotubes decreased further (05/field) (Fig. 3D and E) and there was also reduction in the number of myonuclei per myotube ($\approx$25) thereby indicating inhibited myogenesis (Fig. 3F).

3.6. Low concentration of NaF supplementation induces hypertrophy and at high concentration induces atrophy of myotubes during myogenic differentiation

Myoblasts (C2C12) were cultured to confluence which is required for differentiation and then induced to differentiate in the presence or absence of supplemental NaF. Differentiated myotubes that formed in the presence of 1 ppm NaF were similar to that of untreated control both at 72 h and 96 h time point (Fig. 4A). Myotubes that formed in the presence of 1.5 ppm NaF were larger/hypertrophied at 72 h when compared to control (Fig. 4A). But at the same concentration when the myotubes were cultured for 96 h they were shorter/thicker (Fig. 4A). Further, when the concentration of supplemented NaF was increased to 5 ppm at 72 h, the myotubes were thinner/atrophied, and at 96 h the myotubes were shorter/atrophied (Fig. 4A). Exposure to higher concentrations of NaF such as 10 ppm, 20 ppm, and 40 ppm results in progressive loss of myotubes, without any effect on myoblasts (Fig. S1D).

Morphometric analysis such as myotube length, myotube diameter, and fusion index was calculated. NaF treatment on C2C12 myotubes with 1.5 ppm at 72 h of differentiation, showed a significant increase in the size of myotubes, i.e., increase in diameter and fusion index but there was a decrease in myotube length when compared with 1 ppm NaF and with untreated control (Fig. 4A, B, C). Further at 96 h there was further decrease in myotube length but increase in diameter and fusion index. Hypertrophy of the myotubes was followed by an accumulation of myonuclei in the centre of the myotubes which is a hallmark of hypertrophy (Fig. 4A).

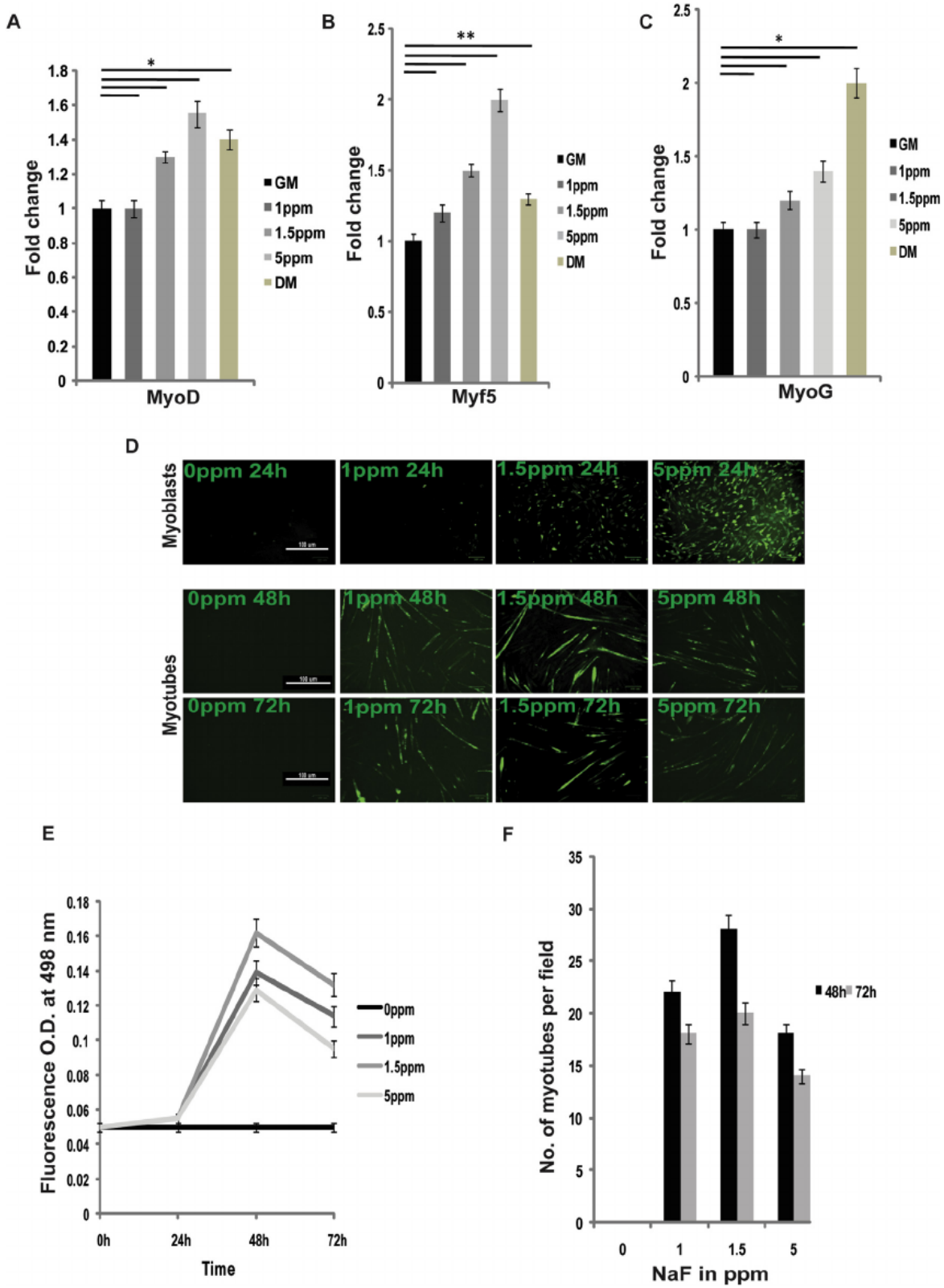

Fig. 2. Effect of NaF on muscle regulatory factors (MRF) and ROS production on C2C12 cells: Cells were cultured in growth medium and differentiation medium in the presence and absence of NaF (1 ppm, 1.5 ppm, 5 ppm). **A, B, C)** Gene expression of MRFs *MyoD, Myf5, and MyoG* 24 h after the cells were treated with different concentrations of NaF *$P < 0.05$. **D)** Fluorescence microscopy images of ROS production in myoblasts and in differentiated myotubes treated with different concentrations of NaF at different time points. **E)** Dose-dependent effect of NaF on ROS production was measured in C2C12 myoblast cells. ROS production was determined using DCFDA-2', 7'—dichlorofluorescin diacetate. Fluorescence intensity was measured at an excitation wavelength of 498 nm and an emission wavelength of 535 nm. **F)** The number of fluorescent myotubes formed per field, calculated from three random fields per treatment. Values are means of ±SD of three experiments. Scale bars: 100 μm.

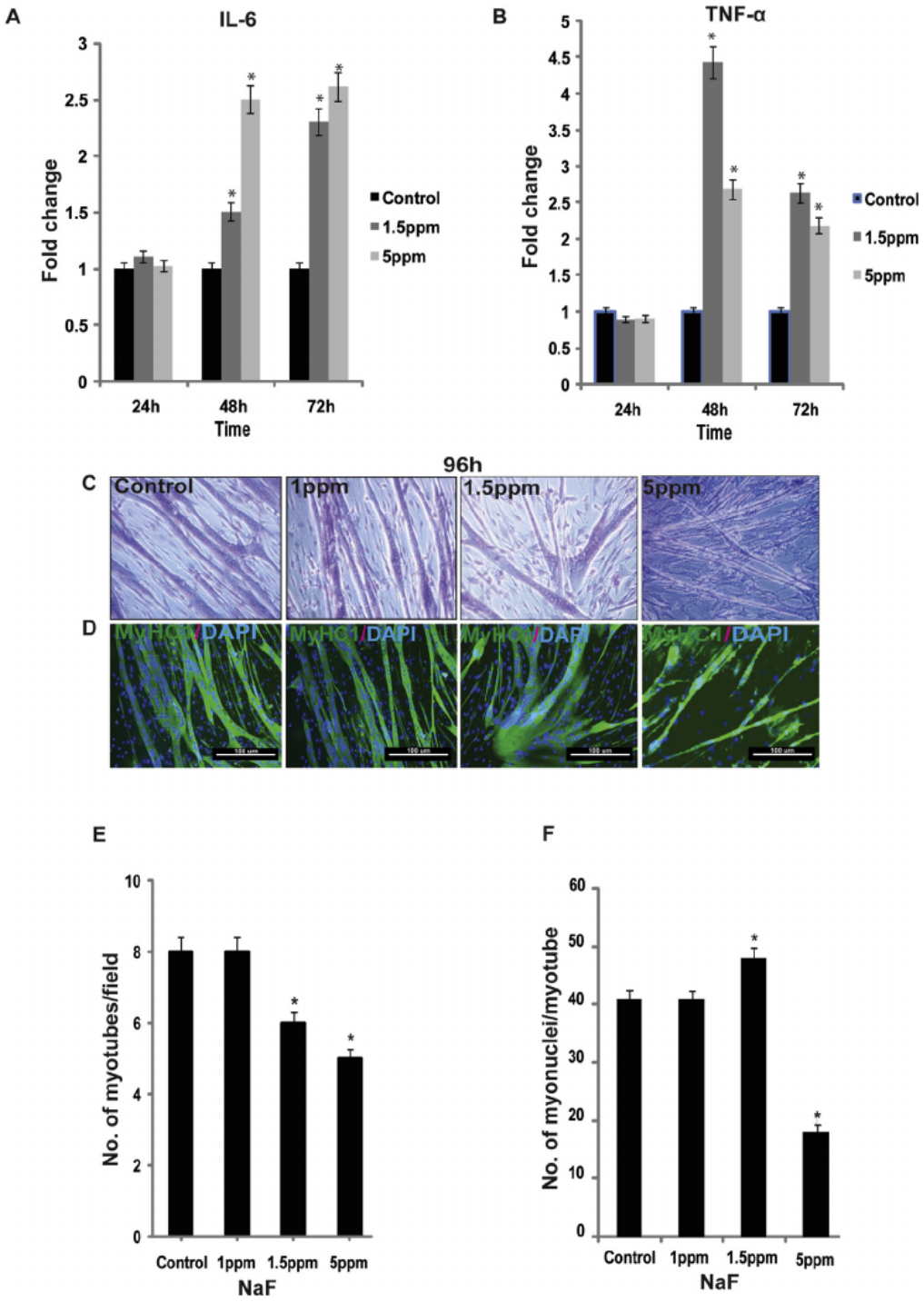

Fig. 3. Effect of NaF on the expression of inflammatory cytokines and morphological changes in differentiated C2C12 myotubes: Cells were cultured in differentiation medium in the presence and absence of NaF (1.5 ppm and 5 ppm). **A and B)** Inflammatory cytokines IL-6 and TNF-α were determined by qRT-PCR for 24 h, 48 h and 72 h *$P < 0.05$. **C**) Morphology of multinucleated myotubes under phase contrast microscopy stained with Giemsa at 96 h of differentiation. **D)** Immunofluorescence staining of myotubes with MyHC1 antibody at 96 h of differentiation. **E)** The number of myotubes formed per field. **F)** The number of myonuclei per myotube, calculated from ten random fields per concentration. Values are means of ±SD of three experiments.*$P < 0.05$.

Myotubes when treated with an increased concentration of NaF, i.e., 5 ppm for 72 h and 96 h during differentiation resulted in myotube atrophy (Fig. 4A). Myotubes length, diameter, and fusion index decreased significantly in the treated concentration and the time point used. There were up to 63% atrophied larger myotubes at 72 h, and 85% atrophied smaller myotubes at 96 h (Fig. 4B). Skeletal muscle hypertrophy and atrophy myotubes dimensions were measured using MyHC1 fluorescence images of the myotubes formed under treatments (Fig. 4A).

3.7. NaF induce hypertrophy of the skeletal muscle via IGF-1/PI3K/Akt signaling pathway

After confirming the hypertrophied myotubes upon induction

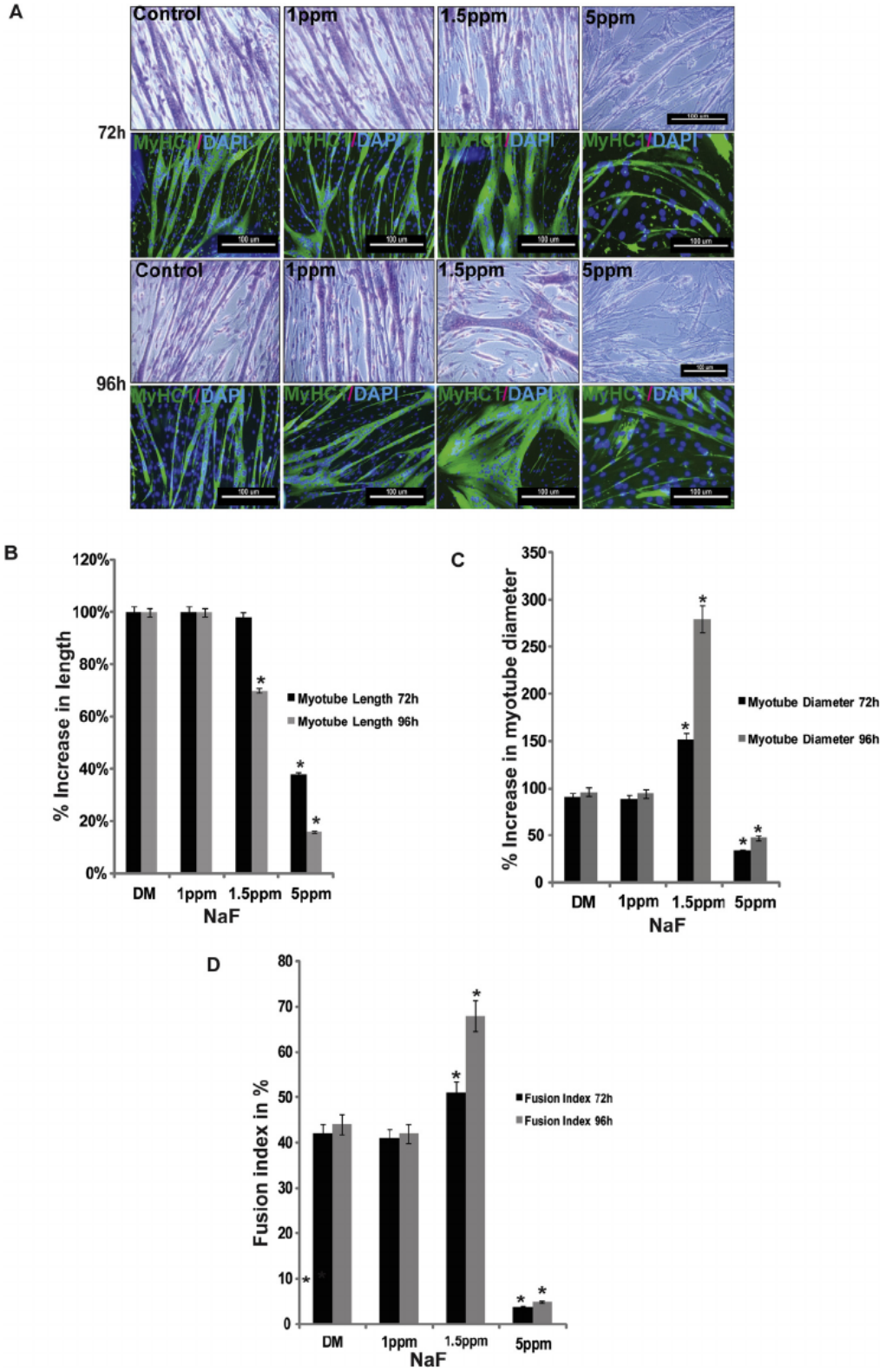

Fig. 4. Morphometric analysis of differentiated C2C12 with hypertrophy and atrophied myotubes 72 h and 96 h: Cells were cultured in differentiation medium in the presence and absence of NaF (1.5 and 5 ppm) for 72 h and 96 h. **A)** Analysis of immunofluorescence (MyHC1) and Giemsa stained myotubes showing hypertrophied (1.5 ppm) and atrophied morphology. Scale bars: 100μm. **B**) Plots representing an increase in myotube length. **C**) Myotube diameter. **D)** Fusion index of NaF treated myotubes compared to differentiation media control.*$P \leq 0.05$. (**Myotubes length:** NaF1.5 ppm 96 h vs. DM 96 h $p \leq 0.01$; 5 ppm 72 h vs. DM 72 h $p \leq 0.01$; 5 ppm 96 h vs. DM 96 h $p \leq 0.05$; **Myotubes diameter:** NaF1.5 ppm 72 h vs. DM 72 h $p \leq 0.01$; 1.5 ppm 96 h vs. DM 96 h $p \leq 0.05$; 5 ppm 72 h vs. DM 72 h $p \leq 0.01$; 5 ppm 96 h vs. DM 96 h $p \leq 0.01$; **Fusion index:** NaF1.5 ppm 72 h vs. DM 72 h $p \leq 0.01$; 1.5 ppm 96 h vs. DM 96 h $p \leq 0.05$; 5 ppm 72 h vs. DM 72 h $p \leq 0.01$; 5 ppm 96 h vs. DM 96 h $p \leq 0.01$).

with NaF (maximum hypertrophy at 1.5 ppm), we went ahead to check the underlying mechanisms of the same. Insulin-like growth factors (IGFs) have been earlier reported to be upregulated along with the inhibition of basic FGF and TGFβ during the differentiation of C2C12 myoblasts under low serum conditions (Yoshiko et al., 2002). Importantly, Insulin-like growth factor-1 (IGF-1) promotes proliferation and differentiation of myoblasts and is the leading anabolic factor in skeletal muscle growth (Yu et al., 2015). Hence, to verify the role of IGF-1 signaling pathway during hypertrophy, we conducted qRT-PCR gene expression analysis and western blot for protein expression on C2C12 cells treated with 1 ppm, 1.5 ppm and 5 ppm of NaF respectively.

NaF (1.5 ppm) treatment on differentiating C2C12 lead to a significant time-dependent upregulation of IGF-1R as assessed by flow cytometry and western blot (Figs. 5A and 6A). 92% of the differentiating C2C12 treated with 1.5 ppm of NaF exhibited positivity for the expression of IGF-1R at 48 h of treatment (Fig. 5A). Time dependent expression of IGF-1R as assessed by the

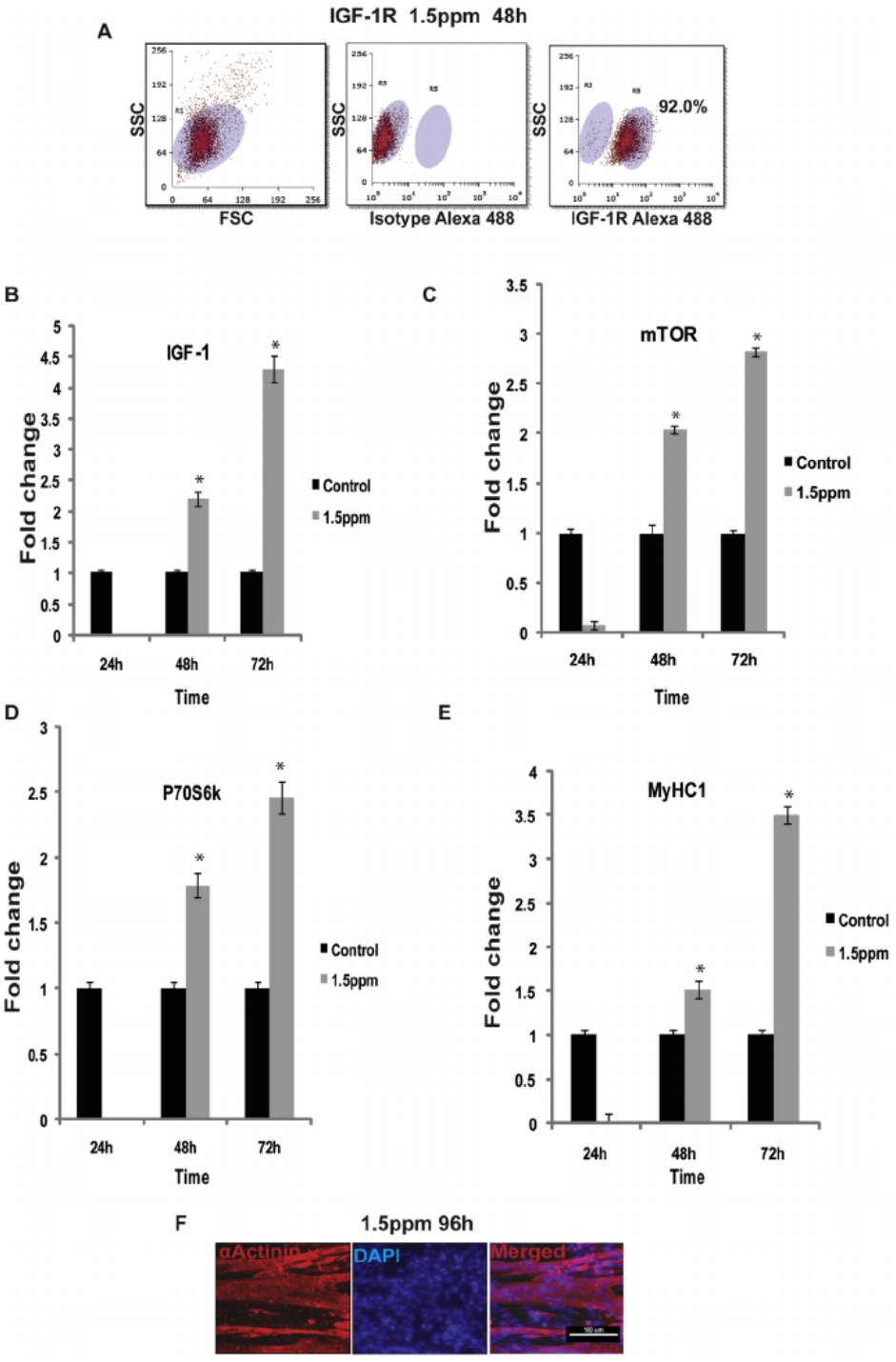

Fig. 5. Low concentration of NaF treatment on differentiating C2C12 myotubes causes activation of the IGF-1 pathway: Cells were cultured in differentiation medium in the presence and absence of NaF (1.5 ppm) for 24 h, 48 h and 72 h. **A)** Flow cytometric analysis of IGF-1R at 48 h of 1.5 ppm NaF treatment. **B**) Gene expression analysis by qRT-PCR, of IGF-1 **C)** mTOR **D)** P70S6K **E)** MyHC-1. **F)** Immunofluorescence staining of hypertrophied myotubes expressing αActinin. Values are means of ±SD of three experiments.*P ˙0.05, compared with DM control.

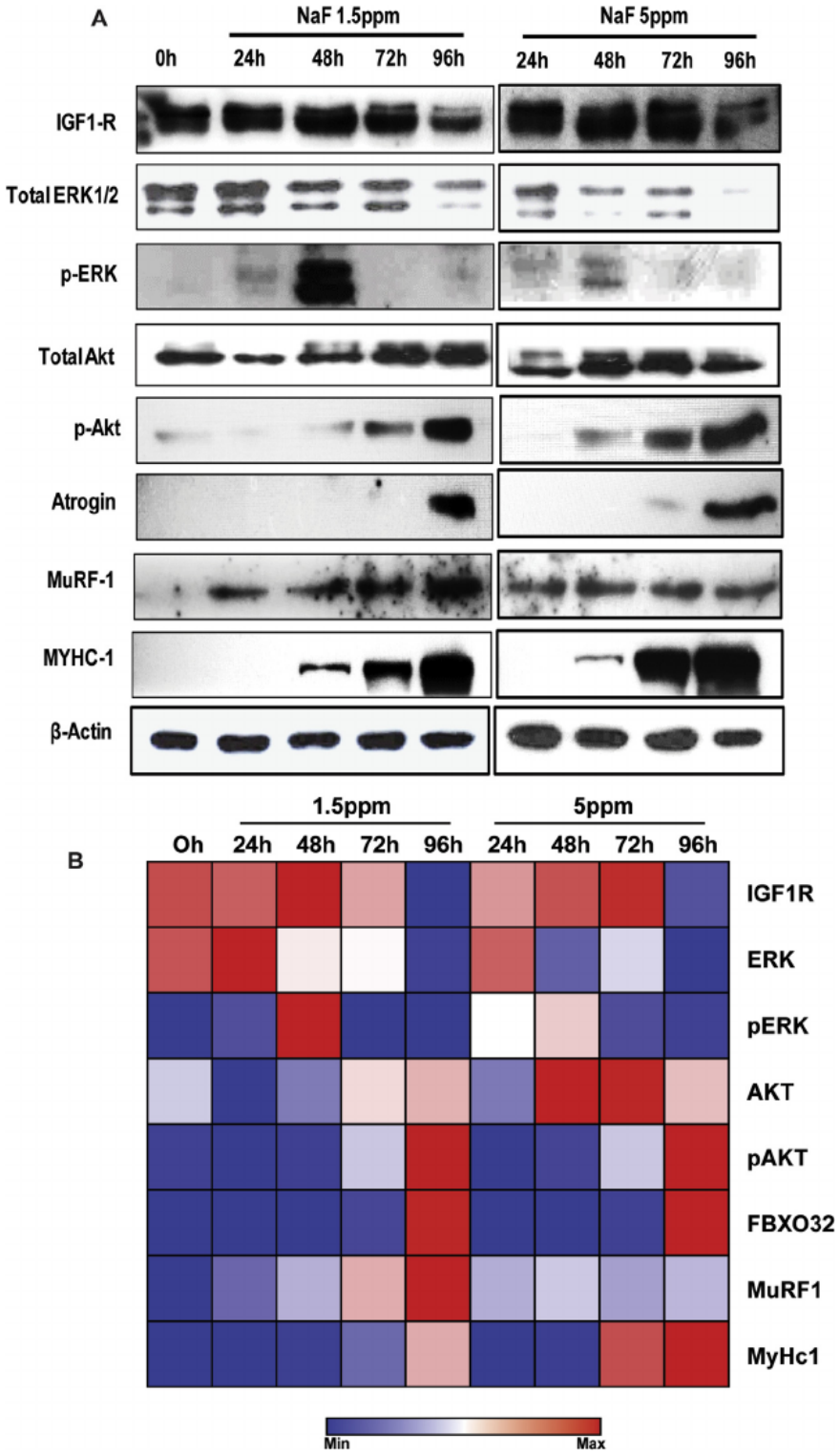

Fig. 6. Effect of NaF on hypertrophy and atrophy pathway protein expression: Cells were cultured in differentiation medium in the presence and absence of NaF (1.5 ppm and 5 ppm) for 24 h, 48 h, 72 h and 96 h. **A**) Protein expression levels of IGF-1R, ERK1/2, pERK1/2, AKT, pAKT, atrogin-1, MURF-1, MyHC-1 were measured by western blot analysis. The experiments were performed three times, and a representative result is shown. **B**) Densitometric analysis of 3 independent experiments is represented in the form of a heat map. The values were normalized to β-actin, and the fold change relative to untreated cells is presented. $^{*}P < 0.05$ compared with the untreated controls.

western blot indicated the highest expression of IGF-1R at 48 h of treatment with 1.5 ppm of NaF (Fig. 6A and B). However, at a still higher concentration of NaF treatment (5 ppm), also time dependent upregulation of IGF-1R was seen at 48 h and 72 h. Moreover, at both the treatments of 1.5 ppm and 5 ppm, there was a decline in IGF-1R protein expression at 96 h thereby indicating a probable reduction in the myogenic differentiation (Fig. 6A and B). Similarly, the gene expression of the IGF-1R ligand, precisely IGF-1, also exhibited a time dependent upregulation at 48 h and 72 h (2 & 4 fold upregulated IGF-1 at 48 h

and 72 h respectively, as compared to controls cells only in differentiation media and no NaF) in differentiating C2C12 treated with 1.5 ppm of NaF (Fig. 5B). Owing to the maximum hypertrophy at 1.5 ppm of NaF treatment, we had restricted the gene expression analysis to this treatment only.

After confirming the role of IGF-1R and IGF-1 during NaF (1.5 ppm) induced hypertrophy in differentiating C2C12 myoblasts, we further assessed the downstream targets of IGF-1 signaling precisely, ERK1/2, AKT, mTOR, and p70S6K. Western blot analyses of total ERK1/2 and total Akt exhibited opposing time-dependent kinetics at 1.5 ppm and 5 ppm of NaF treatment. Precisely, Total ERK1/2 exhibited a downregulation from 48 h onwards in the differentiating C2C12 myotubes treated with both the concentrations of NaF (Fig. 6A and B). Contrarily, total Akt exhibited an upregulation from 48 h onwards in differentiating C2C12 myotubes treated with both the concentrations of NaF (Fig. 6A and B). The highest expression of phosphorylated ERK was observed at 48 h in 1.5 ppm and 5 ppm treatment of NaF respectively. However, the highest expression of phosphorylated Akt was observed at 96 h of both 1.5 ppm and 5 ppm of NaF treatment respectively (Fig. 6). Further, qRT-PCR gene expression analysis of downstream targets, such as mTOR and p70S6K exhibited a respective upregulation by two fold at 48 h when treated with 1.5 ppm of NaF, as compared to the control differentiating myotubes without NaF (Fig. 5C and D). Respective upregulation by ~3 fold and ~2.5 for mTOR and p70S6K at 72 h was observed in 1.5 ppm NaF treated differentiating myotubes (Fig. 5CD). The same results of hypertrophied myotubes and enhanced myogenesis was further corroborated using qRT-PCR gene expression analysis for myosin heavy chain (MyHC1) that exhibited a significant upregulation at 48 h (1.5 fold) and 72 h (3.5 fold) (Fig. 5E) and the immunofluorescence the myotubes expressing sarcomeric αActinin (Fig. 5F).

3.8. Higher concentrations (5 ppm) of NaF caused skeletal muscle atrophy

Treatment with a higher concentration of NaF, i.e., 5 ppm on differentiating C2C12 myotube cultures resulted in the myotubular atrophy in mouse the myoblast cell line (Fig. 7A). Treatment of C2C12 myotube cultures with NaF (5 ppm) induced the loss of muscle proteins and up-regulation of intermediates of the ubiquitin-proteasomal pathway. We analyzed the expression of atrogin-1 and MURF-1, two crucial ubiquitin E3 ligases, which are markers of different forms of skeletal muscle wasting (Lecker et al., 2004). The results (WB, ICC, qRT-PCR) revealed a significant increase of both atrogin-1/FBXO32 at 96 h and MURF-1 in all time points in the C2C12 mouse myoblast cell line treated with 5 ppm NaF (Figs. 6A, 7A and 7B). We also noted that treatment with NaF both with 1.5 ppm and 5 ppm caused a significant increase in the expression of myostatin mRNA at 48 h and 72 h time points in dose and time-dependent manner (Fig. 7C).

Dose (NaF 1.5 ppm and 5 ppm) and time-dependent (24 h, 48 h, and 72 h) expression of myostatin are an indicative of enhanced muscle atrophy at 5 ppm of NaF treatment at 72 h of treatment of C2C12 differentiating myotube cultures. Western blot and qRT-PCR analysis confirmed the upregulation of MyHC1 protein expression in C2C12 mouse myotube cultures treated with NaF 5 ppm (Fig. 7D) at the given time points of 72 h and 96 h respectively indicating the ongoing myogenesis. These data demonstrated that NaF induced myotubular atrophy resulted in the loss of skeletal muscle proteins suggestive of increased protein degradation through the ubiquitin proteasomal system. Further, the role played by sodium fluoride on skeletal muscle myoblasts and myotubes is summarized in (Fig. 8).

4. Discussion

Skeletal muscle is a vital tissue of musculoskeletal system providing support and mobility to an individual. Diet, exercise, age, disease and certain chemical compounds are known to influence muscle hypertrophy or atrophy respectively. Fluoride is an beneficial trace element and promotes cell proliferation at low concentrations in various cell types (Krishnamachari, 1986). NaF has been established for its beneficial role in the skeletal system, precisely bone metabolism as low concentrations support mineralization of bone whereas a high concentration acts adversely (Antonarakis et al., 2014). However, very high doses of NaF are reported to cause adverse effects on the bones leading to apoptosis (Pereira et al., 2017; Gu et al., 2016). Moreover, NaF has also been reported to induce adverse effects on the cardiac muscle via ROS production and NFκβ pathway at very high doses (150 ppm, 300 ppm and 600 ppm) rats (Oyagbemi et al., 2017) and mitochondrial pathway mediated apoptosis *in vitro* in H9c2 cardiomyocytes (Yan et al., 2017). Apart from the adverse effects of high concentrations of NaF on bone cells and cardiac muscle, the role of high and low concentrations of fluoride has never been studied in the skeletal muscle systems-myoblasts or differentiating myotubes.

In this present study, we demonstrate the role NaF on myoblast proliferation, differentiation and its molecular mechanisms by which it induced myotube hypertrophy and atrophy. The main purpose of this study is to understand the beneficial versus harmful effects of NaF intake on skeletal muscle cells using a range of concentrations of NaF in the culture media Moreover, fluoride is known to be an environmental toxicant posing a lot of health problems in fluoride endemic areas in India (Chakraborti et al., 2016). Hence, the range of concentrations of NaF chosen for our study correlated well with the concentrations that are present in natural drinking water in certain fluoride endemic areas of India, in addition to the safe recommended doses.

NaF exhibited varied effects on myoblasts and myotubes. It induced proliferation of C2C12 myoblasts without any cell death in all concentrations (1 ppm-40 ppm; Fig. 1) tested. Increased cell proliferation was observed at 48 h that reached a peak at 72 h causing a change in morphology from cuboidal to spindle shape (Fig. 1F) in C2C12 treated with both 1.5 ppm and 5 ppm concentrations of NaF. Expression of *MyoD* and *Myf5* transcription factors increased gradually with increase in NaF concentration in proliferating myoblasts thereby confirming the proliferation status of the myoblasts. However, when the C2C12 cells were kept in differentiation media along with NaF, the expression of *MyoD* and *Myf5* decreased. Although, the cell numbers continued to show an increase when the proliferating myoblasts were treated with increasing concentrations of NaF from 1 ppm to 40 ppm, the cyclins (Cyclin A2, B1, C, D, E1 and F) exhibited a gradual decrease in a dose-dependent manner at 24 h of treatment of C2C12 proliferating myoblasts, thereby indicating a probable effect of the NaF on the cell cycle checkpoint inhibition. However, further validation experiments need to be conducted to understand the effect of varying concentrations of NaF on cell cycle checkpoint inhibition of proliferating myoblasts.

NaF toxicity promotes ROS production and accumulation, and this inhibits some of the antioxidant enzymes (Kale et al., 1999; Shivarajashankara et al., 2003). Production of ROS by NaF was seen in myoblasts and myotubes (Fig. 2C). Abnormal levels of ROS reportedly leads to the accumulation of mitochondrial DNA defects (mitophagy) mediated through *Parkin* leading to muscle atrophy (Xiao et al., 2017). Similarly, in this study, we had also observed ROS mediated mitophagy mediated through *Parkin* gene when the differentiating C2C12 were treated with high concentrations of NaF.

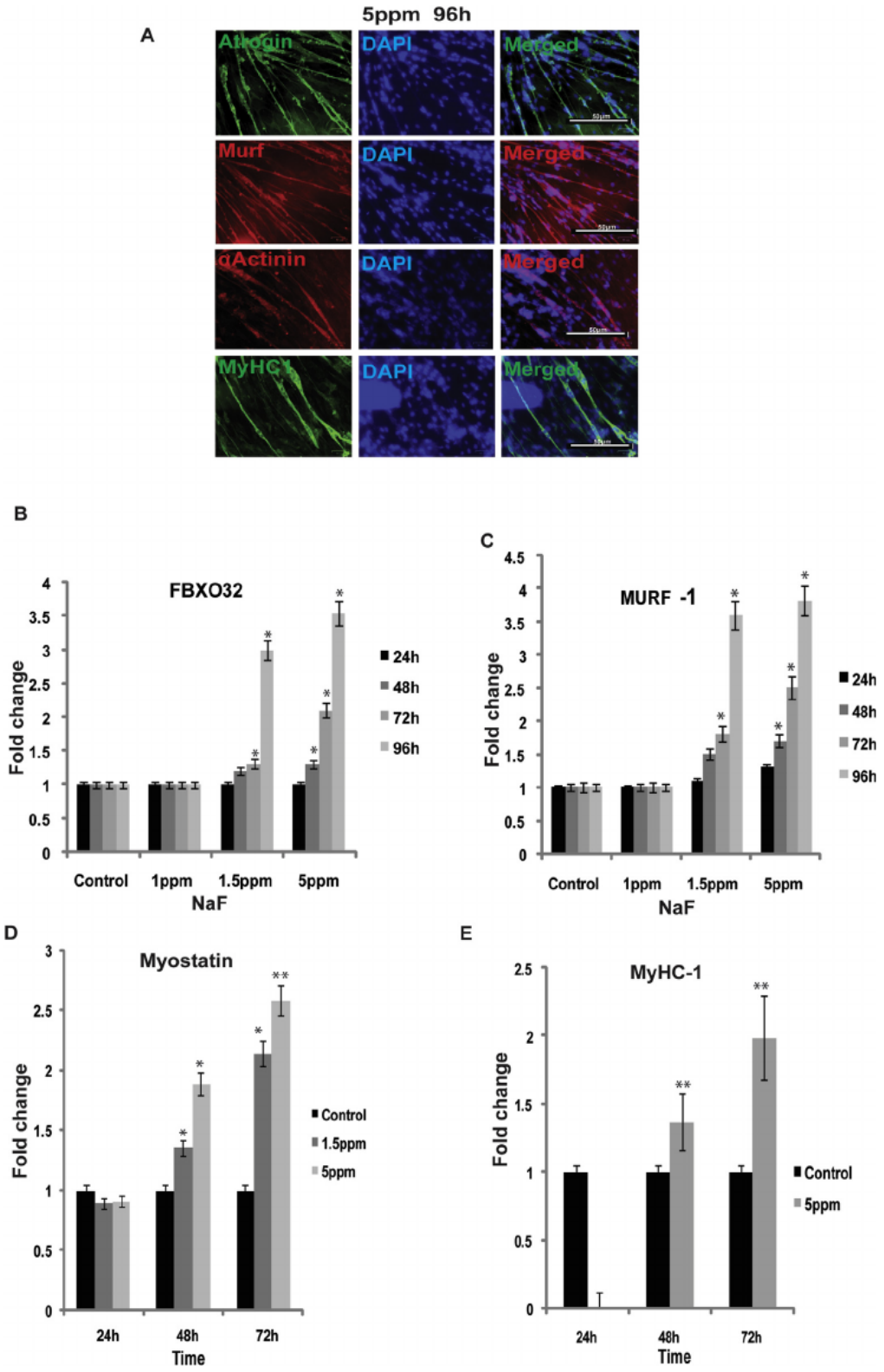

Fig. 7. Higher concentration of NaF treatment on differentiating C2C12 myotubes causes activation of Atrogenes (ubiquitin-proteosome pathway): Cells were cultured in differentiation medium in the presence and absence of NaF (5 ppm) for 24 h, 48 h and 72 h. **A)** Immunofluorescence staining of atrophied myotubes expressing atrogin-1, Murf-1, αActinin, and MyHC-1. Gene expression analysis by qRT-PCR, **B)** FBXO32 **C)** MURF-1 **D)** Myostatin **E)** MyHC-1. Values are means of ±SD of three experiments.*$P < 0.05$, **$P < 0.01$ compared with DM control.

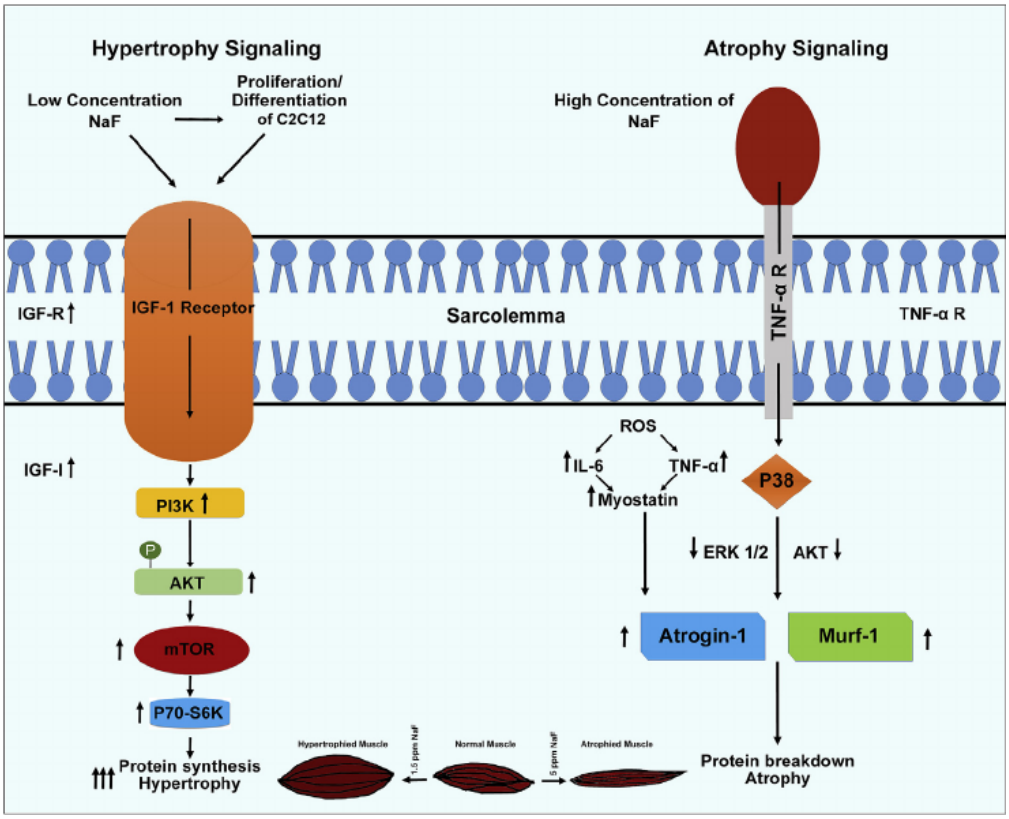

Fig. 8. Schematic representation/mechanism of NaF induced skeletal muscle hypertrophy and atrophy: Low concentration of NaF causes increased proliferation and differentiation of the myoblasts leading to increased IGF-1R and increased endogenous expression of IGF-1 which causes enhanced PI3K/Akt/mTOR/p70S6K signaling pathway leading to hypertrophy of the muscle. Higher concentration of NaF causes atrophy of the skeletal muscle. NaF causes increased ROS production, this, in turn, triggers inflammatory cytokines TNFα and IL-6 to induce myostatin and atrogin-1 expression leading to muscle wasting.

Absence or down-regulation *Mfn2* expression indicates the progression of muscle wasting in NaF treated cells. Our observation correlates well with the earlier work of Xi et al., (2016) reporting Mfn2 induced muscle wasting (Xi et al., 2016). ROS production also causes an increase in inflammatory cytokines, and there seems to be a close relationship between oxidative stress, inflammation and muscle wasting (Sriram et al., 2011; Powers et al., 2005). NaF induced vigorous production of ROS which inhibited the differentiation of C2C12 cells with concomitant expression of myostatin, atrogin-1 along with inflammatory cytokines such as TNF-α and IL-6 expression in cells.

Myostatin had earlier been reported to be the key inducer of muscle atrophy via reduced protein synthesis and enhanced protein degradation (Zhang et al., 2011; Verzola et al., 2011). Hence, it might be possible that myostatin here is acting as a key inducer of muscle atrophy in the presence of NaF due to the reduction in protein synthesis and increase in protein degradation. Furthermore, the effects of inflammatory cytokines and myostatin are closely correlated leading to muscle atrophy. In the current study, NaF generated maximum ROS at a 1.5 ppm concentration at 48 h in C2C12 cells (Fig. 2). In fact, 1.5 ppm of NaF treatment along with a maximum ROS production induced maximum hypertrophy that might be correlated with a balance of antioxidant enzymes present in the myotubes during 1.5 ppm of NaF treatment which forms the future scope of the study. Moreover, at 5 ppm of NaF treatment in differentiating C2C12 myotubes, TNF-α mRNA level decreased both at 48 h and 72 h, which may be attributed due to the myotubes undergoing atrophy (Fig. 2). These results can also be interpreted as, NaF enhances TNF-α level in muscles, which in turn increases myostatin levels and further induces IL-6 production. Similar kind of expression of inflammatory cytokines was also observed in chronic kidney disease (CKD) and intestinal tumors (Zhang et al., 2011; Verzola et al., 2011) (Carson and Baltgalvis, 2010).

Skeletal muscle hypertrophy can be induced by various agents such as betaine, resveratrol, IGF-1, arachidonic acid, folic acid (Senesi et al., 2013; Montesano et al., 2013; Yoshiko et al., 2002; Markworth and Cameron-Smith, 2013; Hwang et al., 2015) by stimulating the phosphatidylinositol-3kinase (PI3K)/Akt pathway. In the current study, we found that NaF at low concentration (1.5 ppm) also caused muscle hypertrophy (Fig. 3C) by activating the PI3K/Akt and Akt/mTOR pathway in differentiating C2C12 myotubes. IGF-1 signaling pathway was, hence, established as the underlying mechanism for hypertrophy in the differentiating C2C12 myotubes in our study resulting in the activation of downstream targets which are required for protein synthesis. IGF1 signaling and its downstream targets have been reported to cause protein synthesis by DeVol et al. (1990). NaF (1.5 ppm) caused excessive proliferation and differentiation of C2C12 myoblasts resulting in endogenous expression of IGF-1 leading to the activation of Akt which is sufficient to induce hypertrophy. Other downstream targets of PI3K/Akt pathway which can cause hypertrophy are mTOR (mammalian target of rapamycin) and p70S6 kinase (Zhang et al., 2000; Montagne et al., 1999). Finally, mTOR seems to play a central role in inducing hypertrophy and protein synthesis. A recent study concludes that NaF induced apoptosis through PI3K/Akt signaling in proliferating C2C12 cells (Zhou et al., 2018). This indicates that PI3K/Akt signaling plays a differential role on myoblasts and differentiated myotubes when stimulated by NaF.

Myostatin expression in skeletal muscle cells brings about rapid catabolic changes in muscle cells by elevating the levels of muscle-

specific E3 ligases, such as atrogin-1and MuRF1 and increasing intracellular ubiquitin–proteosome pathway (McFarlane et al., 2006; Lokireddy et al., 2012). In this case, we have also observed the role of high concentrations of NaF (5 ppm) leading to the expression of myostatin, upregulated muscle-specific E3 ubiquitin ligases such as atrogin-1 and MuRF1, catabolic changes, and hence atrophied myotubes. The rate of protein degradation was significantly increased when compared with control myotubes (Fig. 6). An increase in signaling of TGFβ pathway and a decrease in IGF-I/PI3K/Akt signaling pathway takes place during skeletal muscle wasting (Glass, 2005; Tisdale, 2010; Sandri et al., 2004). In the current study, our results indicated a time-dependent increase of total and phosphorylated Akt at 5 ppm concentrations of NaF in differentiating myotubes with progressive atrophy that is opposite of what has been reported by Sandri et al., (2004) (Fig. 6A). Low levels of Akt coincided with decreased protein synthesis and increase in the activity of FoxO transcription factors which further induce the expression of muscle-specific E3 ligases to enhance skeletal muscle catabolism during cancer cachexia (Sandri et al., 2004; Waddell et al., 2008).

NaF from past few decades is known for its toxic effects on human populations at higher concentrations. There are conflicting reports on the presence of fluoride (safe dose) in drinking water. Ingested fluoride is readily absorbed and gets distributed in the body; highest amount being retained in the bone and teeth (ASTDR, 2003). The occurrence of fluorosis is seen both in younger and aged individuals, the severity of fluoride intake causes changes in the musculoskeletal system such as deformity of the skeleton, degeneration of cartilage and skeletal muscle etc. Further investigations (*in vitro* and *in vivo*) are required to find out the long-term exposure of the safe dose, and exact role played by NaF on skeletal muscle and NaF toxicity reversal mechanisms.

5. Conclusion

Findings from our study indicate that NaF at low concentration can stimulate proliferation and differentiation of myoblasts and require a very high concentration to induce cell death and apoptosis in myoblasts. Furthermore at low concentration NaF causes excessive proliferation of myoblasts and causes hypertrophy of the myotubes during differentiation and can be possibly be used as muscle enhancing factor. At higher concentrations, NaF causes atrophy of the myotubes and can be understood as toxic for muscle growth and development.

Acknowledgments

The authors would like to thank the Yenepoya Research Centre, Yenepoya University Mangalore for its infrastructure and core-facility support for conducting this research. This research was funded by Yenepoya Deemed to be University, India seed grant (YU/SG/059-2017) and grant from Department of Science and Technology, India (DST, EMR/2017/000591) Government of India, awarded to the principal investigator (Sudheer Shenoy P). The authors would also like to thank Dr. Harsha Gowda, Group Leader, QIMR Berghofer Medical Research Institute, University of Queensland Australia for gifting the C2C12 cell line, Anu V. Ranade (Assistant Prof University of Sharjah, UAE) for gifting four antibodies and Prof. Chitta R. Chowdhury for his support, valuable discussion, and inputs on fluoride research.

Appendix A. Supplementary data

Supplementary data to this article can be found online at https://doi.org/10.1016/j.envpol.2018.10.034.

References

Antonio, L.S., Jeggle, P., MacVinish, L.J., et al., 2017. The effect of fluoride on the structure, function, and proteome of a renal epithelial cell monolayer. Environ. Toxicol. 32 (4), 1455–1467.
Antonarakis, G.S., Moseley, R., Waddington, R.J., 2014. Differential influence of fluoride concentration on the synthesis of bone matrix glycoprotein within mineralizing bone cells in vitro. Acta Odontol. Scand. 72 (8), 1066–1069.
Asawa, K., Singh, A., Bhat, N., Tak, M., et al., 2015. Association of temporomandibular joint signs & symptoms with dental fluorosis & skeletal manifestations in endemic fluoride areas of dungarpur district, Rajasthan, India. J. Clin. Diagn. Res. 9 (12), ZC18–21.
ASTDR, 2003. Toxicological Profile for Fluorides, Hydrogen Fluoride, and Fluorine. US Department of Health and Human Services, Public Health Service, Atlanta, GA.
Bailey, K., Chilton, J., Dahi, E., et al., 2006. Fluoride in Drinking-water. World Health Organization, Geneva.
Berkes, C.A., Tapscott, S.J., 2005. MyoD and the transcriptional control of myogenesis. Semin. Cell Dev. Biol. 16 (4–5), 585–595.
Buzalaf, M.A., Whitford, G.M., 2011. Fluoride metabolism. Monogr. Oral Sci. 22, 20–36.
Carson, J.A., Baltgalvis, K.A., 2010. Interleukin 6 as a key regulator of muscle mass during cachexia. Exerc. Sport Sci. Rev. 38 (4), 168–176.
Chakraborti, D., Rahman, M.M., Chatterjee, A., et al., 2016. Fate of over 480 million inhabitants living in arsenic and fluoride endemic Indian districts: magnitude, health, socio-economic effects and mitigation approaches. J. Trace Elem. Med. Biol. 38, 33–45.
Chinoy, N.J., Memon, M.R., 2001. Beneficial effects of some vitamins and calcium on fluoride and aluminium toxicity on gastrocnemius muscle and liver of male mice. Fluoride 34 (1), 21–33.
Dabrowska, E., Letko, R., Balunowska, M., 2006. Effect of sodium fluoride on the morphological picture of the rat liver exposed to NaF in drinking water. Adv. Med. Sci. 51 (Suppl. 1), 91–95.
De Falco, M., De Luca, A., 2006. Involvement of cdks and cyclins in muscle differentiation. Eur. J. Histochem. 50 (1), 19–23.
Denbesten, P., Li, W., 2011. Chronic fluoride toxicity: dental fluorosis. Monogr. Oral Sci. 22, 81–96.
DeVol, D.L., Rotwein, P., Sadow, J.L., et al., 1990. Activation of insulin-like growth factor gene expression during work-induced skeletal muscle growth. Am. J. Physiol. 259 (1 Pt 1), E89–E95.
Dharmagunawardhane, H.A., Malaviarachchi, S.P.K., Burgess, W., 2016. Fluoride content of minerals in gneissic rocks at an area of endemic dental fluorosis in Sri Lanka: estimates from combined petrographic and electron microprobe analysis. Ceylon J Sci 45 (1), 57–66.
Edmunds, W.M., Smedley, P.L., 1996. Groundwater geochemistry and health: an overview. In: Appleton, Fuge, McCall (Eds.), Environmental Geochemistry and Health, vol. 113. Geological Society Special Publication, pp. 91–105.
Feng, D., Huang, H., Yang, Y., et al., 2015. Ameliorative effects of N-acetylcysteine on fluoride-induced oxidative stress and DNA damage in male rats' testis. Mutat. Res. Genet. Toxicol. Environ. Mutagen 792, 35–45.
Ge, Y.M., Ning, H.M., Feng, C.P., et al., 2006. Apoptosis brain cells of offspring rats exposed to high fluoride and low iodine. Fluoride 39 (3), 173–179.
Glass, D.J., 2005. Skeletal muscle hypertrophy and atrophy signaling pathways. Int. J. Biochem. Cell Biol. 37 (10), 1974–1984.
Gomes-Marcondes, M.C., Tisdale, M.J., 2002. Induction of protein catabolism and the ubiquitin-proteasome pathway by mild oxidative stress. Cancer Lett. 180 (1), 69–74.
Gu, X., Han, D., Chen, W., et al., 2016. SIRT1-mediated FoxOs pathways protect against apoptosis by promoting autophagy in osteoblast-like MC3T3-E1 cells exposed to sodium fluoride. Oncotarget 7 (40), 65218.
Hwang, S.Y., Kang, Y.J., Sung, B., et al., 2015. Folic acid promotes the myogenic differentiation of C2C12 murine myoblasts through the Akt signaling pathway. Int. J. Mol. Med. 36 (4), 1073–1080.
Kale, M., Rathore, N., John, S., et al., 1999. Lipid peroxidative damage on pyrethroid exposure and alterations in antioxidant status in rat erythrocytes: a possible involvement of reactive oxygen species. Toxicol. Lett. 105 (3), 197–205.
Kebede, A., Retta, N., Abuye, C., et al., 2016. Dietary fluoride intake and associated skeletal and dental fluorosis in school age children in rural ethiopian rift valley. Int. J. Environ. Res. Publ. Health 13 (8).
Kitzmann, M., Fernandez, A., 2001. Crosstalk between cell cycle regulators and the myogenic factor MyoD in skeletal myoblasts. Cell. Mol. Life Sci. 58 (4), 571–579.
Krishnamachari, K.A., 1986. Skeletal fluorosis in humans: a review of recent progress in the understanding of the disease. Prog. Food Nutr. Sci. 10 (3–4), 279–314.
Kumar, A., Bhatnagar, S., Paul, P.K., 2012. TWEAK and TRAF6 regulate skeletal muscle atrophy. Curr. Opin. Clin. Nutr. Metab. Care 15 (3), 233–239.
Lecker, S.H., Jagoe, R.T., Gilbert, A., et al., 2004. Multiple types of skeletal muscle atrophy involve a common program of changes in gene expression. Faseb. J. 18 (1), 39–51.
Li, J., Wen, C., Yang, S., et al., 1989. A preliminary analysis on the isoenzymes of SLDH from patients with endemic fluorosis. Endem. Dis. Bull. 4, 70–73.
Li, Y.P., Reid, M.B., 2000. NF-kappaB mediates the protein loss induced by TNF-alpha in differentiated skeletal muscle myotubes. Am. J. Physiol. Regul. Integr. Comp. Physiol. 279 (4), R1165–R1170.

Lokireddy, S., Wijesoma, I.W., Sze, S.K., et al., 2012. Identification of atrogin-1-targeted proteins during the myostatin-induced skeletal muscle wasting. Am. J. Physiol. Cell Physiol. 303 (5), C512–C529.
Mantovani, F., Piazza, S., Gostissa, M., et al., 2004. Pin1 links the activities of c-Abl and p300 in regulating p73 function. Mol. Cell. 14 (5), 625–636.
Markworth, J.F., Cameron-Smith, D., 2013. Arachidonic acid supplementation enhances in vitro skeletal muscle cell growth via a COX-2-dependent pathway. Am. J. Physiol. Cell Physiol. 304 (1), C56–C67.
McFarlane, C., Plummer, E., Thomas, M., et al., 2006. Myostatin induces cachexia by activating the ubiquitin proteolytic system through an NF-kappaB-independent, FoxO1-dependent mechanism. J. Cell. Physiol. 209 (2), 501–514.
Montagne, J., Stewart, M.J., Stocker, H., et al., 1999. Drosophila S6 kinase: a regulator of cell size. Science 285 (5436), 2126–2129.
Montesano, A., Luzi, L., Senesi, P., et al., 2013. Resveratrol promotes myogenesis and hypertrophy in murine myoblasts. J. Transl. Med. 11, 310.
Moylan, J.S., Reid, M.B., 2007. Oxidative stress, chronic disease, and muscle wasting. Muscle Nerve 35 (4), 411–429.
Mukhopadhyay, D., Chattopadhyay, A., 2014. Induction of oxidative stress and related transcriptional effects of sodium fluoride in female zebrafish liver. Bull. Environ. Contam. Toxicol. 93 (1), 64–70.
Muller, P., Schmid, K., Warnecke, G., et al., 1992. Sodium fluoride-induced gastric mucosal lesions: comparison with sodium monofluorophosphate. Zeitschrift fur Gastroenterologie 30 (4), 252–254.
Nielsen, F.H., 2009. Micronutrients in parenteral nutrition: boron, silicon, and fluoride. Gastroenterology 137 (5 Suppl. l), S55–S60.
O'Mullane, D.M., Baez, R.J., Jones, S., et al., 2016. Fluoride and oral health. Community Dent. Health 33 (2), 69–99.
Oliver, M.H., Harrison, N.K., Bishop, J.E., et al., 1989. A rapid and convenient assay for counting cells cultured in microwell plates: application for assessment of growth factors. J. Cell Sci. 92 (Pt 3), 513–518.
Oyagbemi, A.A., Omobowale, T.O., Asenuga, E.R., et al., 2017. Sodium fluoride induces hypertension and cardiac complications through generation of reactive oxygen species and activation of nuclear factor kappa beta. Environ. Toxicol. 32 (4), 1089–1101.
Pang, Y.X., Guo, Y.Q., Zhu, P., et al., 1996. The effects of fluoride alone and in combination with selenium, on the morphology and histochemistry of skeletal muscle. Fluoride 29 (2), 59–62.
Park, S., Ajtai, K., Burghardt, T.P., 1999. Inhibition of myosin ATPase by metal fluoride complexes. Biochim. Biophys. Acta 1430 (1), 127–140.
Pereira, H.A., Leite Ade, L., Charone, S., et al., 2013. Proteomic analysis of liver in rats chronically exposed to fluoride. PloS One 8 (9), e75343.
Pereira, A.G., Chiba, F.Y., Mattera, M.S.D.L.C., et al., 2017. Effects of fluoride on insulin signaling and bone metabolism in ovariectomized rats. J. Trace Elem. Med. Biol. 39, 140–146.
Powers, S.K., Kavazis, A.N., DeRuisseau, K.C., 2005. Mechanisms of disuse muscle atrophy: role of oxidative stress. Am. J. Physiol. Regul. Integr. Comp. Physiol. 288 (2), R337–R344.
Rosenkranz, A.R., Schmaldienst, S., Stuhlmeier, K.M., et al., 1992. A microplate assay for the detection of oxidative products using 2',7'-dichlorofluorescin-diacetate. J. Immunol. Methods 156 (1), 39–45.
Sandri, M., Sandri, C., Gilbert, A., et al., 2004. Foxo transcription factors induce the atrophy-related ubiquitin ligase atrogin-1 and cause skeletal muscle atrophy. Cell 117 (3), 399–412.
Sandri, M., 2008. Signaling in muscle atrophy and hypertrophy. Physiology 23, 160–170.
Sartorelli, V., Fulco, M., 2004. Molecular and cellular determinants of skeletal muscle atrophy and hypertrophy. Sci. STKE 2004 (244), re11.
Senesi, P., Luzi, L., Montesano, A., et al., 2013. Betaine supplement enhances skeletal muscle differentiation in murine myoblasts via IGF-1 signaling activation. J. Transl. Med. 11, 174.
Sharples, A.P., Stewart, C.E., 2011. Myoblast models of skeletal muscle hypertrophy and atrophy. Curr. Opin. Clin. Nutr. Metab. Care 14 (3), 230–236.
Shashi, A., Bhushan, B., Bhardwaj, M., 2010. Histochemical pattern of gastrocnemius muscle in fluoride toxicity syndrome. Asia Pacific J. Trop. ed. 136–140.
Shashi, A., Bhushan, B., Sharma, N., 2009. Abnormalities of lipid composition in gastrocnemius muscle of rat exposed to fluoride. Online J. Biotech. Res. 1 (3), 140–143.
Shashi, A., Rana, N., 2016. Ultrastructural study of muscle fibers in experimental fluorosis. J. Basic Appl. Res. 2 (3), 266–271.
Shashi, A., Singh, J., Thapar, S., 1992. Protein degradation in skeletal muscle of rabbit during experimental fluorosis. Fluoride 25, 155–158.
Shashi, A., 1989. Fluoride toxicity and muscular manifestations: histopathological effects in rabbit. Fluoride 22 (72–77).
Shivarajashankara, Y.M., Shivashankara, A.R., Bhat, P.G., et al., 2003. Lipid peroxidation and antioxidant systems in the blood of young rats subjected to chronic fluoride toxicity. Indian J. Exp. Biol. 41 (8), 857–860.
Sriram, S., Subramanian, S., Sathiakumar, D., et al., 2011. Modulation of reactive oxygen species in skeletal muscle by myostatin is mediated through NF-kappaB. Aging Cell 10 (6), 931–948.
Tisdale, M.J., 2010. Cancer cachexia. Curr. Opin. Gastroenterol. 26 (2), 146–151.
Tsunogae, T., Osanai, Y., Owada, M., et al., 2003. High fluorine pargasites in ultrahigh temperature granulites from tonagh island in the Archean Napier complex, east Antarctica. Lithos 70 (1–2), 21–38.
Urbansky, E.T., 2002. Fate of fluorosilicate drinking water additives. Chem. Rev. 102 (8), 2837–2854.
Velica, P., Bunce, C.M., 2011. A quick, simple and unbiased method to quantify C2C12 myogenic differentiation. Muscle Nerve 44 (3), 366–370.
Verzola, D., Procopio, V., Sofia, A., et al., 2011. Apoptosis and myostatin mRNA are upregulated in the skeletal muscle of patients with chronic kidney disease. Kidney Int. 79 (7), 773–782.
Waddell, D.S., Baehr, L.M., van den Brandt, J., et al., 2008. The glucocorticoid receptor and FOXO1 synergistically activate the skeletal muscle atrophy-associated MuRF1 gene. Am. J. Physiol. Endocrinol. Metab. 295 (4), E785–E797.
Wang, H.W., Zhao, W.P., Tan, P.P., et al., 2017. The MMP-9/TIMP-1 system is involved in fluoride-induced reproductive dysfunctions in female mice. Biol. Trace Elem. Res. 178 (2), 253–260.
WHO, 2008. WHO Guidelines for Drinking-water Quality.
Xi, Q.L., Zhang, B., Jiang, Y., et al., 2016. Mitofusin-2 prevents skeletal muscle wasting in cancer cachexia. Oncol. Lett. 12 (5), 4013–4020.
Xiao, B., Goh, J.Y., Xiao, L., et al., 2017. Reactive oxygen species trigger Parkin/PINK1 pathway-dependent mitophagy by inducing mitochondrial recruitment of Parkin. J. Biol. Chem. 292 (40), 16697–16708.
Yan, X., Wang, L., Yang, X., et al., 2017. Fluoride induces apoptosis in H9c2 cardiomyocytes via the mitochondrial pathway. Chemosphere 182, 159–165.
Yin, S., Song, C., Wu, H., et al., 2015. Adverse effects of high concentrations of fluoride on characteristics of the ovary and mature oocyte of mouse. PloS One 10 (6), e0129594.
Yoshiko, Y., Hirao, K., Maeda, N., 2002. Differentiation in C(2)C(12) myoblasts depends on the expression of endogenous IGFs and not serum depletion. Am. J. Physiol. Cell Physiol. 283 (4), C1278–C1286.
Yu, M., Wang, H., Xu, Y., et al., 2015. Insulin-like growth factor-1 (IGF-1) promotes myoblast proliferation and skeletal muscle growth of embryonic chickens via the PI3K/Akt signalling pathway. Cell Biol. Int. 39 (8), 910–922.
Zhang, H., Stallock, J.P., Ng, J.C., et al., 2000. Regulation of cellular growth by the Drosophila target of rapamycin dTOR. Genes Dev. 14 (21), 2712–2724.
Zhang, J., Li, Z., Qie, M., et al., 2016. Sodium fluoride and sulfur dioxide affected male reproduction by disturbing blood-testis barrier in mice. Food Chem. Toxicol. 94, 103–111.
Zhang, L., Rajan, V., Lin, E., et al., 2011. Pharmacological inhibition of myostatin suppresses systemic inflammation and muscle atrophy in mice with chronic kidney disease. Faseb. J. 25 (5), 1653–1663.
Zhang, M., Wang, A., Xia, T., et al., 2008. Effects of fluoride on DNA damage, S-phase cell-cycle arrest and the expression of NF-kappaB in primary cultured rat hippocampal neurons. Toxicol. Lett. 179 (1), 1–5.
Zhou, B.H., Tan, P.P., Jia, L.S., et al., 2018. PI3K/AKT signaling pathway involvement in fluoride induced apoptosis in C2C12 cells. Chemosphere 9 (199), 297–302.
Zohoori, F.V., Innerd, A., Azevedo, L.B., et al., 2015. Effect of exercise on fluoride metabolism in adult humans: a pilot study. Sci. Rep. 5, 16905.